

# Solid-State NMR Spectroscopy of Anionic Framework Aluminophosphates: A New Method to Determine the Al/P Ratio

Dan Zhou,<sup>†</sup> Jun Xu,<sup>‡</sup> Jihong Yu,<sup>\*,†</sup> Lei Chen,<sup>‡</sup> Feng Deng,<sup>\*,‡</sup> and Ruren Xu<sup>†</sup>

State Key Laboratory of Inorganic Synthesis and Preparative Chemistry, College of Chemistry, Jilin University, Changchun 130012, P. R. China, and State Key Laboratory of Magnetic Resonance and Atomic and Molecular Physics, Wuhan Institute of Physics and Mathematics, The Chinese Academy of Sciences, Wuhan 430071, P. R. China

Received: November 2, 2005

A series of anionic framework aluminophosphates, with different Al/P ratios, have been investigated by various solid-state NMR techniques, including  $^{27}\text{Al}$ ,  $^{31}\text{P}$  magic angle spinning (MAS),  $^{27}\text{Al} \rightarrow ^{31}\text{P}$  cross polarization (CP),  $^{27}\text{Al}\{^{31}\text{P}\}$  rotational echo double resonance (REDOR), and  $^{31}\text{P}\{^{27}\text{Al}\}$  transfer of population double resonance (TRAPDOR). Different Al coordinations ( $\text{AlO}_4$ ,  $\text{AlO}_5$ , and  $\text{AlO}_6$ ) and P coordinations ( $\text{PO}_4$ ,  $\text{PO}_3\text{O}_t$ ,  $\text{PO}_2\text{O}_{2t}$ , and  $\text{PO}_b\text{O}_{3t}$ ), where b represents bridging oxygens and t represents terminal oxygens, can be unambiguously determined based on the solid-state NMR spectroscopy. Furthermore, a new method to determine the Al/P ratio of open-framework aluminophosphates has been established, which is useful for the understanding of unknown aluminophosphate structures.

## Introduction

Since the first discovery of microporous aluminophosphates  $\text{AlPO}_4\text{-}n$  ( $n$  denotes a specific structure type),<sup>1</sup> the synthesis of aluminophosphates has attracted great attention because of their potential application in catalysis, adsorption, and separation.<sup>2–4</sup> The aluminophosphate family displays rich structure chemistry,<sup>5</sup> encompassing neutral zeolite-like open frameworks and anionic frameworks with a three-dimensional (3D) open-framework, two-dimensional (2D) layer, one-dimensional (1D) chain, and zero-dimensional (0D) cluster structures.

In contrast to neutral framework  $\text{AlPO}_4\text{-}n$  with an Al/P ratio of exclusive unity, which are constructed from the strict alternation of tetrahedrally coordinated Al and P atoms, anionic framework aluminophosphates show vast structural and compositional diversities with an Al/P ratio of less than unity, owing to the occurrence of coordination numbers greater than four for Al atoms and the existence of terminal P–O bonds. The Al polyhedra include  $\text{AlO}_4$ ,  $\text{AlO}_5$ , and  $\text{AlO}_6$ , and the P tetrahedra include  $\text{PO}_4$ ,  $\text{PO}_3\text{O}_t$ ,  $\text{PO}_2\text{O}_{2t}$ , and  $\text{PO}_b\text{O}_{3t}$  (with b representing bridging oxygens and t terminal oxygens). The diverse linkages of Al polyhedral units and P tetrahedral units via Al–O–P bonds result in various stoichiometries, including  $\text{AlPO}_4(\text{OH})^-$ ,  $\text{AlP}_4\text{O}_{16}^{9-}$ ,  $\text{AlP}_2\text{O}_8^{3-}$ ,  $\text{Al}_2\text{P}_3\text{O}_{12}^{3-}$ ,  $\text{Al}_3\text{P}_4\text{O}_{16}^{3-}$ ,  $\text{Al}_3\text{P}_5\text{O}_{20}^{6-}$ ,  $\text{Al}_4\text{P}_5\text{O}_{20}^{3-}$ ,  $\text{Al}_5\text{P}_6\text{O}_{24}^{3-}$ ,  $\text{Al}_{11}\text{P}_{12}\text{O}_{48}^{3-}$ ,  $\text{Al}_{12}\text{P}_{13}\text{O}_{52}^{3-}$ ,  $\text{Al}_{13}\text{P}_{18}\text{O}_{72}^{15-}$ , and so forth.<sup>5</sup>

High-resolution solid-state NMR spectroscopy, which is sensitive to the local ordering and topology of nuclei environments, has been proven to be an efficient complementary method to X-ray diffraction and has been extensively used in the structural investigations of zeolite structures.<sup>6–13</sup> In the case of aluminosilicate zeolites, the  $^{29}\text{Si}$  chemical shifts display a regular dependence upon the number of  $\text{AlO}_4$  tetrahedra connected to

the  $\text{SiO}_4$  tetrahedron, that is,  $\text{Si}(4\text{Al})$ ,  $\text{Si}(3\text{Al}, 1\text{Si})$ ,  $\text{Si}(2\text{Al}, 2\text{Si})$ ,  $\text{Si}(1\text{Al}, 3\text{Si})$ , and  $\text{Si}(4\text{Si})$ , and the Si/Al ratio can be calculated from the peak areas of the five peaks in the  $^{29}\text{Si}$  spectrum.<sup>14–16</sup> In microporous  $\text{AlPO}_4\text{-}n$ , the correlation between chemical shifts of Al nuclei and P nuclei and mean Al–O–P angles have been reported and applied extensively to the assignment of different resonances.<sup>17,18</sup>

During the past decades, several dipolar-coupling-based solid-state NMR techniques have been developed to ascertain connectivity and internuclear interaction information by reintroducing heteronuclear dipolar coupling between quadrupolar and spin- $1/2$  nuclei in the structural investigation of aluminosilicate and aluminophosphate zeolites.<sup>19–27</sup> These include rotational echo double resonance (REDOR), transferred echo double resonance (TEDOR), transfer of populations double resonance (TRAPDOR), rotational echo adiabatic passage double resonance (REAPDOR), and so forth. Cross polarization (CP) from quadrupolar nuclei to spin- $1/2$  nuclei is also useful for structure studies, because information regarding the bonding can be obtained in a relatively short time.<sup>28,29</sup> Recently, REDOR and TRAPDOR techniques have been employed by Huang et al. to characterize the chemical environments of P and Al in AlPO-based mesostructured lamellar materials, and the average numbers of Al atoms and P atoms in the second coordination spheres for each P and Al site have been estimated.<sup>30</sup>

It is attractive to investigate the solid-state NMR spectroscopy of anionic framework aluminophosphates with rich Al and P coordinations. In this work, a series of anionic framework aluminophosphates with different Al/P ratios have been characterized by various solid-state NMR techniques, including  $^{27}\text{Al}$ ,  $^{31}\text{P}$  MAS,  $^{27}\text{Al} \rightarrow ^{31}\text{P}$  CP/MAS,  $^{27}\text{Al}\{^{31}\text{P}\}$  REDOR, and  $^{31}\text{P}\{^{27}\text{Al}\}$  TRAPDOR NMR. On the basis of the solid-state NMR spectroscopy, the chemical environments of Al and P can be unambiguously determined. Furthermore, a new method to determine the Al/P ratio of open-framework aluminophosphates has been established.

\* To whom correspondence should be addressed. E-mail: jihong@mail.jlu.edu.cn; dengf@wipm.ac.cn.

<sup>†</sup> Jilin University.

<sup>‡</sup> Wuhan Institute of Physics and Mathematics.

**TABLE 1:  $^{27}\text{Al}$  and  $^{31}\text{P}$  Chemical Shifts of Anionic Framework Aluminophosphates Investigated in This Work with Different Al/P Ratios and Al and P Coordination States (numbered 1–11)**

| no. | Al/P ratio | compound  | $^{27}\text{Al}$ NMR shift <sup>a</sup> |                   |                   | $^{31}\text{P}$ NMR shift       |                                  |                                 |                         | ref. |
|-----|------------|---|---|-------------------|-------------------|---------------------------------|----------------------------------|---------------------------------|-------------------------|------|
|     |            |   | AlO <sub>4b</sub>                       | AlO <sub>5b</sub> | AlO <sub>6b</sub> | PO <sub>6</sub> O <sub>3t</sub> | PO <sub>2b</sub> O <sub>2t</sub> | PO <sub>3b</sub> O <sub>t</sub> | PO <sub>4b</sub>        |      |
| 1   | 1/2        | AlPO-CSC  | 40                                      |                   |                   |                                 | −13.8                            |                                 |                         | 31   |
| 2   | 1/2        | AlPO-ESC  | 35                                      |                   |                   | −10.6                           |                                  | −12.7 <sup>b</sup>              |                         | 31   |
| 3   | 2/3        | UT-4  | <b>49</b><br>37.6                       |                   |                   |                                 | −13.1                            | −14.7                           |                         | 39   |
| 4   | 2/3        | [Al <sub>2</sub> P <sub>3</sub> O <sub>10</sub> (OH) <sub>2</sub> ][C <sub>6</sub> NH <sub>8</sub> ]          | 41                                      | 12.3              |                   |                                 |                                  | −20.4                           |                         | 32   |
| 5   | 3/4        | [Al <sub>3</sub> P <sub>4</sub> O <sub>16</sub> ][C <sub>2</sub> NH <sub>8</sub> ] <sub>3</sub>               | <b>32.7</b>                             |                   |                   |                                 |                                  | −20.5<br>−20.7<br>−23           | −21.6                   | 33   |
| 6   | 3/4        | [Al <sub>3</sub> P <sub>4</sub> O <sub>16</sub> ][C <sub>3</sub> N <sub>2</sub> H <sub>5</sub> ] <sub>2</sub> | 38.5                                    | <b>0</b>          |                   |                                 | −14.3                            | −17.5                           | −24.7                   | 34   |
| 7   | 4/5        | Mu-4  | 40                                      | 4.5               |                   |                                 | −13.9                            | −23.6                           | −23.6<br>−29.4<br>−32.6 | 40   |
| 8   | 4/5        | AlPO-HDA  | 41                                      | <b>14</b>         |                   |                                 | −14                              |                                 | −17.8<br>−27.0<br>−29.2 | 35   |
| 9   | 4/5        | AlPO-CJ19   | 44.4<br>39.6                            | 10                | −14.5             |                                 |                                  | −16.7                           | −18.8                   | 36   |
| 10  | 5/6        | JDF-20  | 33                                      |                   |                   |                                 |                                  | −22.7<br>−24.4                  | −30.9                   | 37   |
| 11  | 11/12      | AlPO-CJ11   | 40                                      |                   | −21.4             |                                 |                                  |                                 | −27.7<br>−29.7          | 38   |

<sup>a</sup> The  $^{27}\text{Al}$  chemical shifts are not corrected for second-order quadrupolar effects. <sup>b</sup> The maximum and minimum values of chemical shift ranges for different Al and P coordination states are indicated in bold.

## Experimental Section

**Sample Preparation and Characterization.** The anionic aluminophosphates investigated in this study (numbered 1 to 11) are listed in Table 1. They have different Al/P ratios and Al and P coordination states. The preparations of compounds AlPO-CSC (1), AlPO-ESC (2), [Al<sub>2</sub>P<sub>3</sub>O<sub>10</sub>(OH)<sub>2</sub>][C<sub>6</sub>NH<sub>8</sub>] (4), [Al<sub>3</sub>P<sub>4</sub>O<sub>16</sub>][C<sub>2</sub>NH<sub>8</sub>]<sub>3</sub> (5), [Al<sub>3</sub>P<sub>4</sub>O<sub>16</sub>][C<sub>3</sub>N<sub>2</sub>H<sub>5</sub>]<sub>2</sub> (6), AlPO-HDA (8), AlPO-CJ19 (9), JDF-20 (10), and AlPO-CJ11 (11) were according to the literature methods.<sup>31–38</sup> UT-4 (3), coexisting with UT-5, was first synthesized by using TEG (tetraethylene glycol) as the solvent.<sup>39</sup> In this work, pure UT-4 crystalline phase was obtained by using pyridine as the solvent instead of TEG. Mu-4 (7), first synthesized in the Al<sub>2</sub>O<sub>3</sub>–H<sub>3</sub>PO<sub>4</sub>–DEF (diethylformamide) system, in which DEF acted as both the solvent and template agent,<sup>40</sup> was obtained by using TEG as the solvent and DEA (diethylamine) as the template agent in this work.

The identities of compounds 1–11 were confirmed by X-ray powder diffraction (XRD) analyses, which were performed on a Siemens D5005 diffractometer with Cu K $\alpha$  radiation ( $\lambda$  = 1.5418 Å).

**NMR Experiments.** All NMR experiments were performed on a Varian Infinity-plus 400 spectrometer operating at a magnetic field strength of 9.4 T. The resonance frequencies at this field strength were 161.9 and 104.2 MHz for  $^{31}\text{P}$  and  $^{27}\text{Al}$ , respectively. A Chemagnetics 5 mm triple-resonance MAS probe was employed to acquire all the spectra (with a spinning rate of 8 kHz).

$^{27}\text{Al}$  MAS spectra were acquired using a one-pulse sequence with a short radio frequency (rf) pulse of 0.5  $\mu\text{s}$  (corresponding to a  $\pi/15$  flip angle) and a pulse delay of 1.0 s. Single-pulse  $^{31}\text{P}$  MAS NMR experiments with  $^1\text{H}$  decoupling were performed with a 90 pulse width of 4.9  $\mu\text{s}$ , a 180 s recycle delay, and a  $^1\text{H}$  decoupling strength of 40 kHz. The TRAPDOR experiment is a rotor-synchronized double-resonance technique designed to measure the correlation between two unlike spins involving at least one quadrupolar nucleus.<sup>20,22</sup> In the  $^{31}\text{P}\{^{27}\text{Al}\}$  TRAPDOR

experiment, a spin–echo pulse sequence was applied to the  $^{31}\text{P}$  spins while  $^{27}\text{Al}$  nuclei were irradiated in an alternating fashion. The TRAPDOR fraction is defined by  $(1 - S/S_0)$ , where  $S$  and  $S_0$  are signal intensities in the spectra acquired with and without  $^{27}\text{Al}$ , respectively. All the TRAPDOR experiments were carried out under the following experimental conditions: the rf field for Al irradiation was 58 kHz, the pulse delay was 180 s, and the irradiation time equals multiples of the rotor period (125  $\mu\text{s}$ ). The  $^{27}\text{Al}\{^{31}\text{P}\}$  REDOR experiment was carried out using a standard REDOR pulse sequence,<sup>19</sup> with and without applying rotor-synchronized  $\pi$  pulses to the  $^{31}\text{P}$  channel. In the REDOR experiment including half-integral quadrupolar nuclei, selective pulses ( $\pi/2$  or  $\pi$ ) were employed to excite the central  $|1/2\rangle \leftrightarrow |-1/2\rangle$  transition of  $^{27}\text{Al}$ . The following parameters were used: spinning rate,  $8000 \pm 2$  Hz; weak selective  $\pi/2$  pulse length, 23  $\mu\text{s}$  for  $^{27}\text{Al}$ ;  $\pi$  pulse length, 9.8  $\mu\text{s}$  for  $^{31}\text{P}$ ; pulse delay, 1 s. Since the magnitude of the normalized difference signal ( $\Delta S = S_0 - S$ ) depends on both the strength of the dipole–dipole coupling and the length of the overall dipolar evolution time  $NTr$  (number of rotor cycles times the duration of one rotor period), the REDOR experiments were carried out as a function of  $NTr$ . The Hartmann–Hahn matching condition for  $^{27}\text{Al} \rightarrow ^{31}\text{P}$  CP/MAS experiments was  $\omega_P = 3\omega_{Al} \pm n\omega_r$  ( $n = 1$  or  $2$ ),<sup>41</sup> where  $\omega_P$  and  $\omega_{Al}$  were the rf field strengths applied on the  $^{31}\text{P}$  and  $^{27}\text{Al}$  channels, respectively, and  $\omega_r$  was the spinning rate. The  $^{27}\text{Al} \rightarrow ^{31}\text{P}$  CP/MAS experimental optimization was carried out on molecular sieve AlPO<sub>4</sub>-5, and the optimized matching condition was as follows:  $\omega_P = 43$  kHz,  $\omega_{Al} = 17$  kHz, and  $\omega_r = 8$  kHz. The contact time for cross-polarization was 2.0 ms. The  $^{31}\text{P}$  and  $^{27}\text{Al}$  chemical shifts were referenced to 85% H<sub>3</sub>PO<sub>4</sub> and 1 M Al(NO<sub>3</sub>)<sub>3</sub> solutions, respectively.

## Results and Discussion

**1.  $^{27}\text{Al}$  NMR Experiments.** In anionic aluminophosphates, there are three types of Al coordinations, that is, AlO<sub>4</sub>, AlO<sub>5</sub>, and AlO<sub>6</sub>. Compounds 1–11 contain three kinds of Al chemical

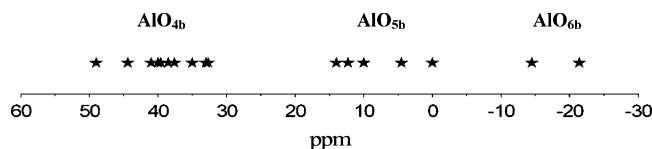


**Figure 1.** Relationship of different Al coordinations and  $^{27}\text{Al}$  chemical shifts of compounds 1–11.

environments, including  $\text{AlO}_{4b}$ ,  $\text{AlO}_{5b}$ , and  $\text{AlO}_{6b}$ , with all vertex oxygens connected to phosphorus. In AIPO-CSC (1), AIPO-ESC (2), UT-4 (3),  $[\text{Al}_3\text{P}_4\text{O}_{16}][\text{C}_2\text{NH}_8]_3$  (5), and JDF-20 (10), the Al coordination environments are exclusively  $\text{AlO}_{4b}$ ; in  $[\text{Al}_2\text{P}_3\text{O}_{10}(\text{OH})_2][\text{C}_6\text{NH}_8]$  (4),  $[\text{Al}_3\text{P}_4\text{O}_{16}][\text{C}_3\text{N}_2\text{H}_5]_2$  (6), Mu-4 (7), and AIPO-HDA (8), they are  $\text{AlO}_{4b}$  and  $\text{AlO}_{5b}$ ; and in AIPO-CJ11 (11), they are  $\text{AlO}_{4b}$  and  $\text{AlO}_{6b}$ . AIPO-CJ19 (9), reported in our recent paper,<sup>36</sup> as we know, is the first aluminophosphate which includes three kinds of Al coordinations ( $\text{AlO}_{4b}$ ,  $\text{AlO}_{5b}$ , and  $\text{AlO}_{6b}$ ) with all oxygen atoms connected to the P atoms.

**$^{27}\text{Al}$  MAS NMR.** The measured  $^{27}\text{Al}$  chemical shifts of compounds 1–11 are summarized in Table 1. These NMR results and their assignments to the specified aluminum are consistent with the results given by single-crystal structure analyses. The chemical shifts corresponding to  $\text{AlO}_{4b}$  fall in the range from 49 to 32 ppm, those corresponding to  $\text{AlO}_{5b}$  in the range from 14 to 0 ppm, and those corresponding to  $\text{AlO}_{6b}$  in the range from -14 to -22 ppm. The relationship of different Al coordinations and  $^{27}\text{Al}$  chemical shifts is demonstrated in Figure 1. It is obvious that, for these anionic framework aluminophosphates,  $\text{AlO}_{4b}$ ,  $\text{AlO}_{5b}$ , and  $\text{AlO}_{6b}$  correspond to different chemical shift ranges, respectively.

**$^{27}\text{Al}\{^{31}\text{P}\}$  REDOR NMR.**  $^{27}\text{Al}\{^{31}\text{P}\}$  REDOR experiments are performed on compounds 1–11 to investigate the strength of an aluminum–phosphorus dipolar interaction for different Al coordinations. For heteronuclear dipolar-coupling-based double-resonance techniques, in the limit of short dipolar evolution times, the slope of the  $\Delta S/S_0$  vs evolution time curve (denoted REDOR curve) depends sensitively on the strength of heteronuclear ( $I$ – $S$ ) dipolar-coupling interaction (i.e., the number of  $S$  spins and internuclear  $I$ – $S$  distances).<sup>30,42,43</sup> In open-framework aluminophosphate systems with strictly alternating aluminum and phosphorus atoms, the average distance between neighbor Al and P atoms is 3.1 Å. Therefore, the initial slope of the  $^{27}\text{Al}\{^{31}\text{P}\}$  REDOR curve only correlates with the number of Al atoms bonded to P. Figure 2 shows the  $^{27}\text{Al}\{^{31}\text{P}\}$  REDOR curves for four-coordinated Al of AIPO-CSC (1) (the signal at 40 ppm), five-coordinated Al of  $[\text{Al}_2\text{P}_3\text{O}_{10}(\text{OH})_2][\text{C}_6\text{NH}_8]$  (4) (the signal at 12.3 ppm), and six-coordinated Al of AIPO-CJ11 (11) (the signal at -21.4 ppm), respectively, and the evolution time is limited to 0.75 ms (corresponding to six rotor periods). It is noteworthy that the three REDOR curves are separated very well, implying that these Al atoms have a different number of P nuclei in the second coordination sphere. The slope of the REDOR curves of the three Al coordinations has an order of  $\text{AlO}_{6b} > \text{AlO}_{5b} > \text{AlO}_{4b}$ . The initial parts of  $\Delta S/S_0$  vs evolution time plots are independent of the exact geometry involved but only dependent on the number of P atoms bonded to Al.<sup>30,44</sup> For instance, the octahedral  $\text{Al}(\text{OP})_4(\text{H}_2\text{O})_2$  unit and tetrahedral  $\text{Al}(\text{OP})_4$  unit will exhibit the same REDOR behavior as  $\text{AlO}_{4b}$ .<sup>30</sup>  $^{27}\text{Al}\{^{31}\text{P}\}$  REDOR experiments can provide a complete assignment on the Al chemical environments.

**$^{31}\text{P}$  NMR Experiments.** In open-framework aluminophosphates, all the P atoms are tetrahedrally coordinated in the form of  $\text{PO}_{4b}$ ,  $\text{PO}_{3b}\text{O}_t$ ,  $\text{PO}_{2b}\text{O}_{2t}$ , and  $\text{PO}_b\text{O}_{3t}$ . Compounds 1–11 contain all the four types of chemical environments. In AIPO-

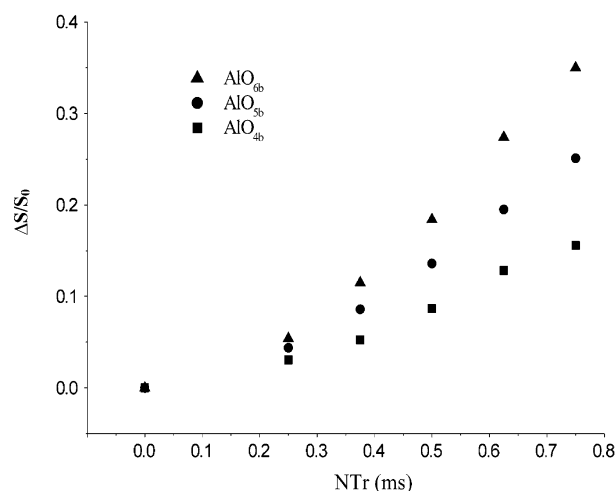


**Figure 2.**  $^{27}\text{Al}\{^{31}\text{P}\}$  REDOR fraction ( $\Delta S/S_0$ ) as a function of evolution time  $NTr$  (number of rotor cycles times duration of one rotor period) for  $\text{AlO}_{4b}$  in AIPO-CSC,  $\text{AlO}_{5b}$  in  $[\text{Al}_2\text{P}_3\text{O}_{10}(\text{OH})_2][\text{C}_6\text{NH}_8]$ , and  $\text{AlO}_{6b}$  in AIPO-CJ11. An MAS spinning speed of 8 kHz was used.

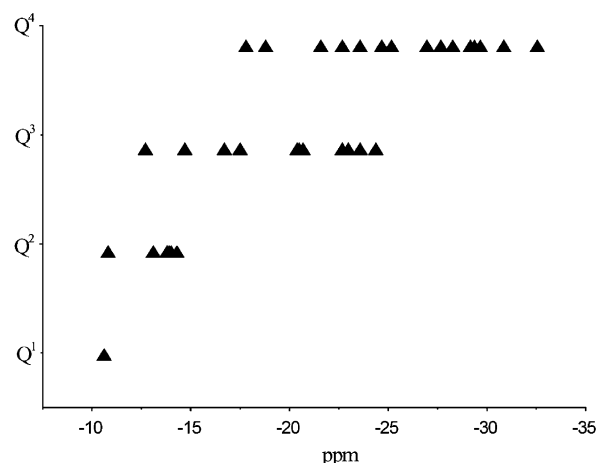


**Figure 3.** Relationship of different P coordinations and  $^{31}\text{P}$  chemical shifts of compounds 1–11.

CSC (1),  $[\text{Al}_3\text{P}_4\text{O}_{16}][\text{C}_2\text{NH}_8]_3$  (5), and AIPO-CJ11 (11), the P coordination environments are  $\text{PO}_{2b}\text{O}_{2t}$ ,  $\text{PO}_{3b}\text{O}_t$ , and  $\text{PO}_{4b}$ , respectively; in AIPO-ESC (2), they are  $\text{PO}_b\text{O}_{3t}$  and  $\text{PO}_{3b}\text{O}_t$ ; in UT-4 (3), they are  $\text{PO}_{2b}\text{O}_{2t}$  and  $\text{PO}_{3b}\text{O}_t$ ; in AIPO-HDA (8), they are  $\text{PO}_{2b}\text{O}_{2t}$  and  $\text{PO}_{4b}$ ; in AIPO-CJ19 (9) and JDF-20 (10), they are  $\text{PO}_{3b}\text{O}_t$  and  $\text{PO}_{4b}$ ; and in  $[\text{Al}_2\text{P}_3\text{O}_{10}(\text{OH})_2][\text{C}_6\text{NH}_8]$  (4),  $[\text{Al}_3\text{P}_4\text{O}_{16}][\text{C}_3\text{N}_2\text{H}_5]_2$  (6), and Mu-4 (7), they are  $\text{PO}_{2b}\text{O}_{2t}$ ,  $\text{PO}_{3b}\text{O}_t$ , and  $\text{PO}_{4b}$ , respectively.

**$^{31}\text{P}$  MAS NMR.** The measured  $^{31}\text{P}$  chemical shifts of compounds 1–11 are listed in Table 1, and the  $^{31}\text{P}$  NMR results and their assignments to the specified phosphorus are consistent with the single-crystal structure analyses. In general, the chemical shifts of P nuclei corresponding to  $\text{PO}_{4b}$  ( $Q^4$ ),  $\text{PO}_{3b}\text{O}_t$  ( $Q^3$ ),  $\text{PO}_{2b}\text{O}_{2t}$  ( $Q^2$ ), and  $\text{PO}_b\text{O}_{3t}$  ( $Q^1$ ) units shift in turn from upfield to downfield with the bridging oxygen atoms connected to P decreasing, owing to a smaller shield effect. Figure 3 shows the relationship of different P chemical environments and  $^{31}\text{P}$  chemical shifts for compounds 1–11. In contrast to the separate chemical shift ranges for different Al coordinations, the chemical shift ranges for different P coordination forms are partially overlapped.  $\text{PO}_{4b}$  units correspond to chemical shifts falling in the range from -17.8 to -32.6 ppm, which is similar to that for  $\text{P}(\text{OAl})_4$  in the neutral framework  $\text{AlPO}_4$ ,<sup>45–47</sup>  $\text{PO}_{3b}\text{O}_t$  in the range from -12.7 to -24.4 ppm,<sup>36,48,49</sup> and  $\text{PO}_{2b}\text{O}_{2t}$  in the

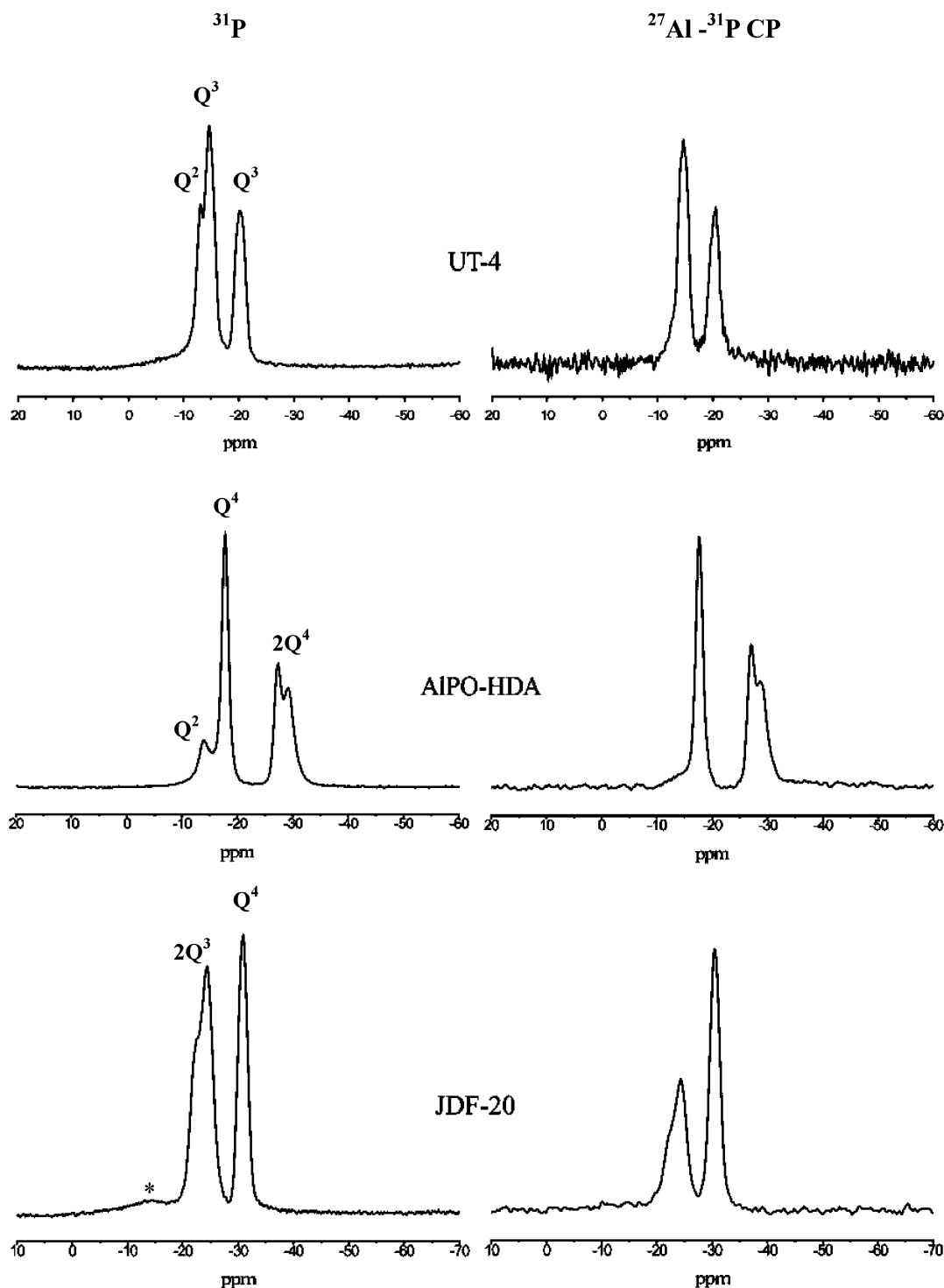


**Figure 4.**  $^{31}\text{P}$  (left) and  $^{27}\text{Al} \rightarrow ^{31}\text{P}$  CP/MAS NMR spectra (right) of UT-4 (top), AIPO-HDA (middle), and JDF-20 (bottom). The asterisk means minor impurity.

range from  $-10.8$  to  $-14.3$  ppm.<sup>32</sup> The chemical shift value of the  $\text{PO}_b\text{O}_{3t}$  unit in AIPO-ESC is  $-10.6$  ppm.<sup>31</sup> The overlapped chemical shift ranges indicate that the assignment of P coordinations cannot be obtained solely on the basis of  $^{31}\text{P}$  chemical shifts.

**$^{27}\text{Al} \rightarrow ^{31}\text{P}$  CP/MAS NMR.** The  $^{27}\text{Al} \rightarrow ^{31}\text{P}$  CP/MAS NMR experiment, with cross-polarization from the quickly relaxing quadrupolar spins, is efficient to give the most direct information regarding the connectivity of aluminum nuclei with phosphorus nuclei and is used extensively to characterize the structure of aluminophosphate molecular sieves.<sup>28,29</sup> For microporous aluminophosphate materials, the enhancement factor of the  $^{31}\text{P}$

signal due to cross-polarization increases as the number of aluminum atoms bonded to the  $\text{PO}_4$  group increases.

$^{27}\text{Al} \rightarrow ^{31}\text{P}$  CP/MAS NMR experiments are performed on compounds 1–11, with selected representative  $^{31}\text{P}$  and  $^{27}\text{Al} \rightarrow ^{31}\text{P}$  CP/MAS NMR spectra shown in Figure 4. In the case of UT-4 (top), the  $^{31}\text{P}$  MAS NMR spectrum consists of three signals at  $-13.1$ ,  $-14.7$ , and  $-20.4$  ppm, corresponding to one P coordination of  $\text{PO}_{2b}\text{O}_{2t}$  ( $\text{Q}^2$ ) and two  $\text{PO}_{3b}\text{O}_t$  ( $\text{Q}^3$ ), respectively. By  $^{27}\text{Al} \rightarrow ^{31}\text{P}$  CP/MAS NMR, it is obvious that, compared with the intensity of the signals at  $-14.7$  and  $-20.4$  ppm, the intensity of the signal at  $-13.1$  ppm decreases significantly and the signal is nearly invisible, owing to one



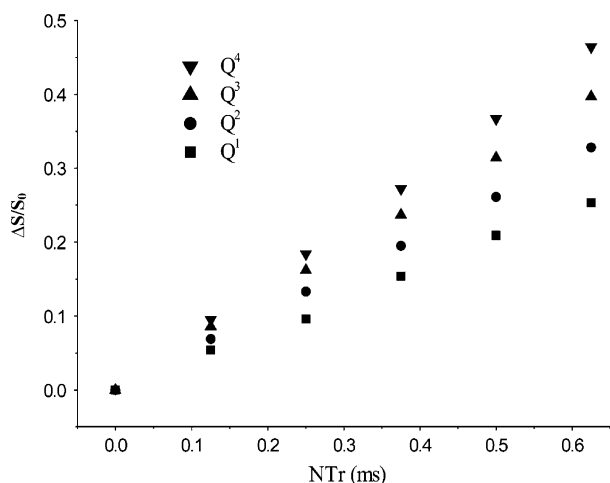


**Figure 5.**  $^{31}\text{P}\{^{27}\text{Al}\}$  TRAPDOR fraction ( $\Delta S/S_0$ ) as a function of evolution time  $NTr$  for  $\text{PO}_4\text{O}_{3i}$  in AIPO-ESC,  $\text{PO}_{2b}\text{O}_{2t}$  in  $[\text{Al}_2\text{P}_3\text{O}_{10}(\text{OH})_2][\text{C}_6\text{NH}_8]$ ,  $\text{PO}_{3b}\text{O}_t$  in  $[\text{Al}_3\text{P}_4\text{O}_{16}][\text{C}_3\text{N}_2\text{H}_5]_2$ , and  $\text{PO}_{4b}$  in AIPO-CJ19 (the signal at  $-25.2$  ppm). An MAS spinning speed of 8 kHz was used.

less bonding of Al and P. Another two examples from AIPO-HDA (middle) and JDF-20 (bottom) present the same results. These examples indicate that  $^{27}\text{Al} \rightarrow ^{31}\text{P}$  CP/MAS NMR spectroscopy is sensitive to the different bondings of Al and P. Therefore, for an unknown aluminophosphate phase, it can be employed to ascertain whether the different  $^{31}\text{P}$  signals in the  $^{31}\text{P}$  MAS NMR spectrum correspond to the same coordination form or not.

However,  $^{27}\text{Al} \rightarrow ^{31}\text{P}$  CP/MAS NMR cannot give information on the number of Al atoms bonded to P. Provided an unknown aluminophosphate phase with the same  $^{31}\text{P}$  chemical shifts with AIPO-HDA (see Figure 4), it is uncertain that the signals at  $-14.0$  and  $-17.8$  ppm are (a)  $\text{PO}_{4b}$  and  $\text{PO}_{3b}\text{O}_t$ , (b)  $\text{PO}_{4b}$  and  $\text{PO}_{2b}\text{O}_{2t}$ , or (c)  $\text{PO}_{3b}\text{O}_t$  and  $\text{PO}_{2b}\text{O}_{2t}$ , because the signal at  $-14.0$  ppm locates at the overlapped chemical shift range of  $\text{PO}_{3b}\text{O}_t$  and  $\text{PO}_{2b}\text{O}_{2t}$  and the signal at  $-17.8$  ppm locates at the overlapped chemical shift range of  $\text{PO}_{4b}$  and  $\text{PO}_{3b}\text{O}_t$ . In another situation when only one  $^{31}\text{P}$  signal exists, which locates at the overlapped chemical shift range of two different P coordinations, the  $^{27}\text{Al} \rightarrow ^{31}\text{P}$  CP experiment will not work, either. For example, in the case of AIPO-CSC (1), one  $^{31}\text{P}$  signal at  $-13.8$  ppm lies within the overlapped chemical shift range of  $\text{PO}_{3b}\text{O}_t$  and  $\text{PO}_{2b}\text{O}_{2t}$ . Therefore, the chemical shift value alone gives no indication of the actual number of Al neighbors attached to a P site. To solve this problem, further experiments have to be carried out to better characterize the P local environments.

**$^{31}\text{P}\{^{27}\text{Al}\}$  TRAPDOR NMR.** In contrast to  $^{27}\text{Al}\{^{31}\text{P}\}$  REDOR by using  $\pi$  pulses during the spin-echo experiment,  $^{31}\text{P}\{^{27}\text{Al}\}$  TRAPDOR is designed to measure the dipolar coupling of heteronuclear involving at least one quadrupolar nucleus by using continuous irradiation pulses.<sup>27,30</sup> To investigate the strength of the phosphorus–aluminum dipolar interaction for different P coordination forms,  $^{31}\text{P}\{^{27}\text{Al}\}$  TRAPDOR experiments are performed on compounds 1–11 and the evolution time is limited to 0.625 ms (corresponding to five rotor periods). The plots of the  $^{31}\text{P}\{^{27}\text{Al}\}$  TRAPDOR fraction ( $\Delta S/S_0$ ) vs evolution time (denoted TRAPDOR curve) for four kinds of P coordination forms in four compounds are shown in Figure 5. It is obvious that, for different P coordination forms, the slopes of the TRAPDOR curves are well separated. The slope of the TRAPDOR curves of the four P environments has an order of  $\text{PO}_{4b} > \text{PO}_{3b}\text{O}_t > \text{PO}_{2b}\text{O}_{2t} > \text{PO}_b\text{O}_{3t}$ . This result is consistent with that reported by Huang et al. on the assignment

of the P chemical environments of AIPO-based mesostructured lamellar materials.<sup>30</sup> The slope ranges for the four P coordination forms of all P signals in compounds 1–11 are 0.72–0.8 for  $\text{PO}_{4b}$ , 0.60–0.63 for  $\text{PO}_{3b}\text{O}_t$ , 0.5–0.53 for  $\text{PO}_{2b}\text{O}_{2t}$ , and 0.41 for  $\text{PO}_b\text{O}_{3t}$  (one case in AIPO-ESC). The above experiments indicate that the combination of the  $^{31}\text{P}$  chemical shift ranges,  $^{27}\text{Al} \rightarrow ^{31}\text{P}$  CP, and  $^{31}\text{P}\{^{27}\text{Al}\}$  TRAPDOR can help to distinguish different P chemical environments.

There is an interesting phenomenon in the course of  $^{31}\text{P}\{^{27}\text{Al}\}$  TRAPDOR experiments for Mu-4 (7) and AIPO-HDA (8). In the  $^{31}\text{P}$  MAS NMR spectrum of Mu-4 (Supporting Information Figure S1), the signal at  $-23.6$  ppm corresponds to two kinds of P coordination forms,  $\text{PO}_{4b}$  and  $\text{PO}_{3b}\text{O}_t$ , which cannot be resolved with a spinning speed of 8 kHz. However, in the  $^{31}\text{P}\{^{27}\text{Al}\}$  TRAPDOR experiment, the two P coordination forms can be well discriminated. The two P signals exhibit the same TRAPDOR behavior with  $\text{PO}_{4b}$  ( $Q^4$ ) and  $\text{PO}_{3b}\text{O}_t$  ( $Q^3$ ), respectively. In contrast to Mu-4, in the  $^{31}\text{P}$  MAS NMR spectrum of AIPO-HDA, the signal at  $-17.8$  ppm corresponds to two distinct  $\text{PO}_{4b}$  sites. In the  $^{31}\text{P}\{^{27}\text{Al}\}$  TRAPDOR experiment, only one signal (at  $-17.8$  ppm) can be resolved and the slope of the TRAPDOR curve of this signal is similar to that of  $\text{PO}_{4b}$  ( $Q^4$ ), implying that the two P sites experience the same magnitude of dipolar interaction with neighboring Al atoms. This result is consistent with the fact that the two P sites have a similar P chemical environment. The above results indicate that the  $^{31}\text{P}\{^{27}\text{Al}\}$  TRAPDOR experiment is efficient to distinguish different P chemical environments, as well as to identify the same P chemical environment.

**3. New Method to Determine the Al/P Ratio of Open-Framework Aluminophosphates.** Although open-framework compounds are highly crystalline and their structures are often highly symmetrical, there are still difficulties in determining their crystal structures only by diffraction techniques. When they are microcrystalline with particle dimensions of only a few micrometers, the application of single-crystal diffraction analysis is limited. Solid-state NMR, which is sensitive to local orderings, can give valuable complementary information about the framework structure, and this is our principal motivation to determine the coordinations of Al and P of open-framework aluminophosphates by solid-state NMR techniques. In this study, the combination of  $^{27}\text{Al}/^{31}\text{P}$  chemical shifts,  $^{27}\text{Al}\{^{31}\text{P}\}$  REDOR,  $^{27}\text{Al} \rightarrow ^{31}\text{P}$  CP/MAS NMR, and  $^{31}\text{P}\{^{27}\text{Al}\}$  TRAPDOR NMR techniques have been employed to characterize different Al and P coordinations in a series of known anionic framework aluminophosphate compounds, and we believe that, for an unknown aluminophosphate structure, this method is also applicable.

The relationship between the Al/P ratios and the Al and P coordination states has been found to satisfy the following eq 1<sup>5</sup>

$$\sum_i m_{\text{AlO}ib} \times i_{\text{AlO}ib} = \sum_j n_{\text{PO}jb} \times j_{\text{PO}jb} \quad (1)$$

where  $i(j)$  is the number of bridging oxygens coordinated to Al(P),  $m(n)$  is the number of  $\text{AlO}ib$  ( $\text{PO}jb$ ) coordination,  $\sum m_{\text{AlO}ib}/\sum n_{\text{PO}jb} = \text{Al/P}$ ,  $i = 4, 5$ , and 6, corresponding to  $\text{AlO}_4$ ,  $\text{AlO}_5$ , and  $\text{AlO}_6$  coordinations, respectively, and  $j = 1, 2, 3$ , and 4, corresponding to  $\text{PO}_4$  tetrahedra with one, two, three, and four bridging oxygens, respectively. The quantification of different Al coordination can be obtained by the combination of  $^{27}\text{Al}$  MQMAS NMR spectrum and the simulation of  $^{27}\text{Al}$  MAS spectrum using the DMFIT program,<sup>36,50</sup> and the quantification

of different P site populations can be obtained by the deconvolution of  $^{31}\text{P}$  MAS spectrum with Gaussian lines.

On the basis of the coordinations of Al and P and the quantification of each kind of coordination, the Al/P ratio can be determined from eq 1. An example from JDF-20 is present to illustrate the analysis process. In the  $^{27}\text{Al}$  MAS NMR spectrum of JDF-20 (Supporting Information Figure S2), the resonances lie within a typical chemical shift range of four-coordinated aluminum nuclei (the asymmetric line shape of the signal is due to the presence of distinct crystallographically aluminum atoms), which is also proven by the  $^{27}\text{Al}\{^{31}\text{P}\}$  REDOR experiment result. In the  $^{31}\text{P}$  MAS NMR spectrum of JDF-20 (see Figure 4), three signals at  $-22.7$ ,  $-24.4$ , and  $-30.9$  ppm are ascribed to  $\text{PO}_{3b}\text{O}_{1t}$ ,  $\text{PO}_{3b}\text{O}_t$ , and  $\text{PO}_{4b}$ , respectively, with an intensity ratio of 1:1:1, as a result of the combination of chemical shift ranges (Figure 3),  $^{27}\text{Al} \rightarrow ^{31}\text{P}$  CP (Figure 4), and  $^{31}\text{P}\{^{27}\text{Al}\}$  TRAPDOR (Supporting Information Figure S2). Suppose that  $m_{\text{AlO}_{1b}}$  is  $x$  and  $n_{\text{PO}_{3b}}$  is  $y$ , and sequentially, the occupancy fractions of  $\text{PO}_{3b}\text{O}_t$  and  $\text{PO}_{4b}$  are  $(2y/3)$  and  $(y/3)$ , respectively. Consequently,  $i_{\text{AlO}_{4b}}$  is 4,  $j_{\text{PO}_{3b}\text{O}_t}$  is 3, and  $j_{\text{PO}_{4b}}$  is 4. Thus, eq 1 becomes

$$x \times 4 = (2y/3) \times 3 + (y/3) \times 4$$

So

$$\text{Al/P} = \sum m_{\text{AlO}_{1b}} / \sum n_{\text{PO}_{3b}} = x/y = 5/6$$

This is a new method to determine the Al/P ratio of framework aluminophosphates, and it is applicable to deduce the Al/P ratio of an unknown aluminophosphate phase. Compared with traditional chemical analysis methods, it has the advantage to detect the Al/P ratio of the framework, which gets rid of the influence from an amorphous phase or extraframework Al and P atoms existing in the product. Similarly, this method holds for all metal phosphates which possess similar structure construction manner with open-framework aluminophosphates.

## Conclusions

A series of anionic framework aluminophosphates, with different Al/P ratios, have been studied by various solid-state NMR techniques, and the combination of  $^{27}\text{Al}$  MAS,  $^{27}\text{Al}\{^{31}\text{P}\}$  REDOR,  $^{31}\text{P}$  MAS,  $^{27}\text{Al} \rightarrow ^{31}\text{P}$  CP/MAS NMR, and  $^{31}\text{P}\{^{27}\text{Al}\}$  TRAPDOR techniques can provide more detailed structural information on both the Al coordinations ( $\text{AlO}_{4b}$ ,  $\text{AlO}_{5b}$ , and  $\text{AlO}_{6b}$ ) and P coordinations ( $\text{PO}_{4b}$ ,  $\text{PO}_{3b}\text{O}_t$ ,  $\text{PO}_{2b}\text{O}_{2t}$ , and  $\text{PO}_{6b}\text{O}_{3t}$ ). The number of Al (or P) atoms in the second coordination sphere for P (or Al) atoms can be unambiguously determined by using TRAPDOR and REDOR techniques. In terms of the relationship between the coordination states and Al/P ratios found for open-framework aluminophosphates, a new method to determine the Al/P ratio of open-framework aluminophosphates based on NMR has been established, which is useful for the understanding of unknown aluminophosphate structures. We are currently developing a computational method to solve the aluminophosphate structure combined with NMR and XRD analyses. The specified Al and P units determined by NMR can be assembled by AASBU (automated assembly of secondary building units) computational method<sup>51</sup> under possible space groups suggested by XRD analysis. Solid-state NMR techniques have demonstrated their powerful strength in the structural investigation of zeolite and related open-framework materials.

**Acknowledgment.** This work is supported by the National Natural Science Foundation of China and the State Basic Research Project of China (G2000077507).

**Supporting Information Available:** Figures showing  $^{31}\text{P}$  MAS NMR spectra,  $^{31}\text{P}\{^{27}\text{Al}\}$  TRAPDOR experiments,  $^{31}\text{P}$  spin-echo, TRAPDOR, and TRAPDOR difference spectra of Mu-4 and AlPO-HDA and  $^{27}\text{Al}$  MAS NMR spectrum and  $^{31}\text{P}\{^{27}\text{Al}\}$  TRAPDOR fraction of JDF-20. This material is available free of charge via the Internet at <http://pubs.acs.org>.

## References and Notes

- (1) Wilson, S. T.; Lok, B. M. C.; Messina, A.; Cannan, T. R.; Flanigen, E. M. *J. Am. Chem. Soc.* **1982**, *104*, 1146.
- (2) Meier, W. H.; Olson, D. H.; Baerlocher, C. *Atlas of Zeolite Structure Types*; Elsevier: London, 2001.
- (3) Bennett, J. M.; Dytrych, W. J.; Pluth, J. J.; Richardson, J. W.; Smith, J. V., Jr. *Zeolites* **1986**, *6*, 349.
- (4) Thomas, J. M.; Raja, R.; Sankar, G.; Bell, R. G. *Acc. Chem. Res.* **2001**, *34*, 191.
- (5) Yu, J.; Xu, R. *Acc. Chem. Res.* **2003**, *36*, 481.
- (6) Chen, F.; Deng, F.; Cheng, M.; Yue, Y.; Ye, C.; Bao, X. *J. Phys. Chem. B* **2001**, *105*, 9426.
- (7) Taulelle, F.; Pruski, M.; Amoureux, J. P.; Lang, D.; Bailly, A.; Huguenard, C.; Haouas, M.; Gérardin, C.; Loiseau, T.; Férey, G. *J. Am. Chem. Soc.* **1999**, *121*, 12148.
- (8) Huang, Y. N.; Machado, D.; Kirby, C. W. *J. Phys. Chem. B* **2004**, *108*, 1855.
- (9) Peng, L.; Chupas, P.; Grey, C. *J. Am. Chem. Soc.* **2004**, *126*, 12254.
- (10) Deng, F.; Yue, Y.; Ye, C. H. *J. Phys. Chem. B* **1998**, *102*, 5252.
- (11) Lim, K.; Jousse, F.; Auerbach, S.; Grey, C. *J. Phys. Chem. B* **2001**, *105*, 9918.
- (12) Blackwell, C. S.; Patton, R. L. *J. Phys. Chem.* **1984**, *88*, 6135.
- (13) Mali, G.; Taulelle, F. *Chem. Commun.* **2004**, 868.
- (14) Lippmaa, E.; Mägi, M.; Samoson, A.; Grimmer, A. R.; Engelhardt, G. *J. Am. Chem. Soc.* **1980**, *102*, 4889.
- (15) Lippmaa, E.; Mägi, M.; Samoson, A.; Tarmak, M.; Engelhardt, G. *J. Am. Chem. Soc.* **1981**, *103*, 4992.
- (16) Fyfe, C. A.; Feng, Y.; Grondey, H.; Kokotailo, G. T.; Gies, H. *Chem. Rev.* **1991**, *91*, 1525.
- (17) Müller, D.; Jahn, E.; Ladwig, G.; Haubenreisser, U. *Chem. Phys. Lett.* **1984**, *109*, 332.
- (18) Tuel, A.; Gramlich, V.; Baerlocher, Ch. *Microporous Mesoporous Mater.* **2001**, *47*, 217.
- (19) Gullion, T.; Schaefer, J. J. *Magn. Reson.* **1989**, *81*, 196.
- (20) Van Eck, E. R. H.; Janssen, R.; Mass, W. E. J. R.; Veeman, W. S. *Chem. Phys. Lett.* **1990**, *174*, 428.
- (21) Hing, A. W.; Vega, S.; Schaefer, J. J. *Magn. Reson.* **1992**, *96*, 205.
- (22) Grey, C. P.; Vega, A. J. *J. Am. Chem. Soc.* **1995**, *117*, 8232.
- (23) Gullion, T. *Chem. Phys. Lett.* **1995**, *246*, 325.
- (24) Fyfe, C. A.; Wong-Moon, K. C.; Huang, Y.; Grondey, H.; Mueller, K. T. *J. Phys. Chem.* **1995**, *99*, 8707.
- (25) Ba, Y.; He, J.; Ratcliffe, C. I.; Ripmeester, J. A. *J. Am. Chem. Soc.* **1999**, *121*, 8387.
- (26) Bailly, A.; Amoureux, J. P.; Wiench, J. W.; Pruski, M. *J. Phys. Chem. B* **2001**, *105*, 773.
- (27) Luo, Q.; Deng, F.; Yuan, Z.; Yang, J.; Zhang, M.; Yue, Y.; Ye, C. *J. Phys. Chem. B* **2003**, *107*, 2435.
- (28) Fyfe, C. A.; Grondey, H.; Mueller, K. T.; Wong-Moon, K. C.; Markus, T. *J. Am. Chem. Soc.* **1992**, *114*, 5876.
- (29) Fyfe, C. A.; Mueller, K. T.; Grondey, H.; Wong-Moon, K. C. *J. Phys. Chem.* **1993**, *97*, 13484.
- (30) Huang, Y. N.; Yan, Z. M. *J. Am. Chem. Soc.* **2005**, *127*, 2731.
- (31) Wang, K.; Yu, J.; Li, C.; Xu, R. *Inorg. Chem.* **2003**, *42*, 4597.
- (32) Yu, J.; Sugiyama, K.; Hiraga, K.; Togashi, N.; Terasaki, O.; Tanaka, Y.; Nakata, S.; Qiu, S.; Xu, R. *Chem. Mater.* **1998**, *10*, 3636.
- (33) Gao, Q. M.; Li, B. Z.; Chen, J. S.; Li, S. G.; Xu, R. R. *J. Solid State Chem.* **1997**, *129*, 37.
- (34) Yu, J.; Williams, I. D. *J. Solid State Chem.* **1998**, *136*, 141.
- (35) Yu, J.; Sugiyama, K.; Zheng, S.; Qiu, S.; Chen, J.; Xu, R.; Sakamoto, Y.; Terasaki, O.; Hiraga, K.; Light, M.; Hursthouse, M. B.; Thomas, J. M. *Chem. Mater.* **1998**, *10*, 1208.
- (36) Zhou, D.; Chen, L.; Yu, J.; Li, Y.; Yan, W.; Deng, F.; Xu, R. *Inorg. Chem.* **2005**, *44*, 4391.
- (37) Huo, Q.; Xu, R.; Li, S.; Ma, Z.; Thomas, J. M.; Jones, R. H.; Chippindale, A. M. *J. Chem. Soc., Chem. Commun.* **1992**, 875.
- (38) Wang, K.; Yu, J.; Shi, Z.; Miao, P.; Yan, W.; Xu, R. *J. Chem. Soc., Dalton Trans.* **2001**, 1809.

- (39) Oliver, S.; Kuperman, A.; Lough, A.; Ozin, G. A. *Chem. Commun.* **1996**, 1761.
- (40) Vidal, L.; Gramlich, V.; Patarin, J.; Gabelica, Z. *Eur. J. Solid State Inorg. Chem.* **1998**, 35, 545.
- (41) Vega, S. *J. Magn. Reson.* **1992**, 96, 50.
- (42) Chan, J. C. C.; Bertmer, M.; Eckert, H. *J. Am. Chem. Soc.* **1999**, 121, 5238.
- (43) van Eck, E. R. H.; Kentgens, A. P. M.; Kraus, H.; Prins, R. *J. Phys. Chem.* **1995**, 99, 16080.
- (44) Bertmer, M.; Eckert, H. *Solid State Nucl. Magn. Reson.* **1999**, 15, 139.
- (45) Caldarelli, S.; Meden, A.; Tuel, A. *J. Phys. Chem. B* **1999**, 103, 5477.
- (46) Jelinek, R.; Chmelka, B. F.; Wu, Y.; Grandinetti, P. J.; Pines, A.; Barrie, P. J.; Klinowski, J. *J. Am. Chem. Soc.* **1991**, 113, 4097.
- (47) Blackwell, C. S.; Patton, R. L. *J. Phys. Chem.* **1988**, 92, 3965.
- (48) Vidal, L.; Marichal, C.; Gramlich, V.; Patarin, J.; Gabelica, Z. *Chem. Mater.* **1999**, 11, 2728.
- (49) Tuel, A.; Gramlich, V.; Baerlocher, Ch. *Microporous Mesoporous Mater.* **2002**, 56, 119.
- (50) Massiot, D.; Fayon, F.; Capron, M.; King, I.; Le Calvé, S.; Alonso, B.; Durand, J.-O.; Bujoli, B.; Gan, Z.; Hoatson, G. *Magn. Reson. Chem.* **2002**, 40, 70.
- (51) Mellot-Draznieks, C.; Férey, G.; Schön, C.; Cancarevic, Z.; Jansen, M. *Chem.—Eur. J.* **2002**, 8, 4102.